High-Resolution Excited-State Photoelectron Spectroscopy of the Lower Rydberg States of Jet-Cooled C_2H_4 and C_2D_4

R. A. Rijkenberg and W. J. Buma*

Faculty of Science, Institute of Molecular Chemistry, University of Amsterdam, Nieuwe Achtergracht 127-129, 1018 WS Amsterdam, The Netherlands

Received: October 3, 2001; In Final Form: January 7, 2002

High-resolution (2+1) resonance-enhanced excited-state photoelectron spectroscopy on supersonic jet expansions of pure C_2H_4 and C_2D_4 has been employed to investigate the spectroscopy and dynamics of the lowest excited $1^1B_{3u}(\pi,3s)$ Rydberg state, as well as the $1^1B_{1g}(\pi,3p_y)$, $1^1B_{2g}(\pi,3p_z)$, and $2^1A_g(\pi,3p_x)$ Rydberg states of ethylene. In combination with ab initio calculations, this approach has for the $1^1B_{3u}(\pi,3s)$ Rydberg state confirmed the majority of previous assignments in the two-photon excitation spectrum but, at the same time, has demonstrated that the hypothesis of a vibronic coupling between this state and the Jahn−Teller distorted $1^1B_{2g}(\pi^*,3s)$ state should be discarded. The resonances on which this hypothesis was based are in the present study shown to arise from excitation of the $\nu_3(a_g)$ vibrational mode. For the 3p Rydberg manifold, the present study has for the first time been able to determine unambiguously the 0−0 transitions to all three $(\pi,3p)$ Rydberg states and to disentangle the vibrational development of the practically degenerate $1^1B_{1g}(\pi,3p_y)$ and $1^1B_{2g}(\pi,3p_z)$ Rydberg states. Upon the basis of these assignments, it has been shown that the $2^1A_g(\pi,3p_x)$ Rydberg state is significantly more twisted around the central CC double bond upon excitation from the ground state than the other two $(\pi,3p)$ Rydberg states. Although a priori argued to be difficult to detect, the present study does not give evidence for previous suggestions in the literature on the coupling of the $1^1B_{1u}(\pi,\pi^*)$ valence and the $1^1B_{3u}(\pi,3s)$ or the $1^1B_{1g}(\pi,3p_y)$ Rydberg states. However, the photoelectron spectra obtained for ionization via the lower Rydberg manifold of both C_2H_4 and C_2D_4 show unambiguously the absence of extensive coupling between the lower excited Rydberg states.

I. Introduction

Molecular systems containing rodlike organic building blocks functionalized by specific substituents at one or both of the termini positions constitute one of the primary areas of interest in the field of organic chemistry dedicated to the development of functionalized materials. The advantage of these organic materials is the possibility to fine-tune the chemical structure, and thus the desired property, by way of synthesis, making them highly suitable candidates within application areas such as photonics and molecular electronics. One such a class of materials with significant potential is built upon oligo(cyclohexilydenes).[1−3] Recent excited-state photoelectron spectroscopic studies[4] on their structural unit, 1,1′-bicyclohexylidene, have strongly suggested that its peculiar spectroscopic properties[5,6] ultimately find their origin in vibronic coupling interactions between the Rydberg manifold and the underlying continua of the valence state(s) of ethylene.[7−13]

The spectroscopy of the lower excited states of ethylene, in particular in relation to vibronic coupling, has in the past been the subject of many experimental and theoretical studies. Despite the vast amount of knowledge that has been acquired by now, we found in our efforts to elucidate the spectroscopic properties of excited states in 1,1′-bicyclohexylidene in particular, and alkylated mono-olefins in general, that some rather fundamental questions on the composition of the wave functions of the lower excited Rydberg states were still unanswered. We have therefore reinvestigated these states with excited-state photoelectron spectroscopy. This spectroscopic technique is very powerful when nonadiabatic interactions between electronically excited states are considered.[14−16] The possibility to disperse the photoelectrons produced in the resonance enhanced multiphoton ionization (REMPI) process according to their kinetic energies enables the characterization of the intermediate state from which ionization occurs, e.g., is it a "pure" vibronic state or is it coupled to one or more other vibronically excited states.[14,16] A second aspect relevant for the present study is that excited-state photoelectron spectroscopy in principle should be able to unravel qualitatively, and in some cases quantitatively, the electronic character of the intermediate state from which ionization occurs, e.g., Rydberg versus valence character.[17]

The coupling of electronically excited states of ethylene has been the subject of several theoretical investigations[7−13,18−20] discussing the interaction between the Rydberg manifold and the (π,π^*) valence state. In this respect, especially the electronic properties of the $1^1B_{1u}(\pi,\pi^*)$ valence state have been the focus of a large number of theoretical studies employing a wide range of ab initio techniques.[7−12,18−32] Because the (π,π^*) valence state and $(\pi,3d_\pi)$ Rydberg state have the same nodal structure, Mulliken[7] argued that the unperturbed (π,π^*) and $(\pi,3d_\pi)$ wave functions cannot coexist for ethylene. Instead, the 1^1B_{1u} valence state of ethylene consists of a linear combination of the (π,π^*) and the $(\pi,3d_\pi)$ wave functions, and the next $^1B_{1u}$ state is the $(\pi,4d_\pi)$ Rydberg state. Buenker and Peyerimhoff[8] hold another view: according to them, the unperturbed (π,π^*) and $(\pi,3d_\pi)$ wave functions coexist separately, but they are subject to extensive configuration mixing in the planar conformation,

* To whom correspondence should be addressed. E-mail: wybren@fys.chem.uva.nl. Fax: (31)-20−525 6456/6422.

10.1021/jp013714k CCC: $22.00
Published on Web 03/14/2002

which diminishes, however, upon twisting around the C=C bond. This mixing of character resulting in a more diffuse valence state has been the subject of several computational studies concentrating on the out-of-plane spatial extension $\langle x^2 \rangle$ of the valence state in the planar conformation.[18,21,25−32] The most recent results report a value for the 1^1B_{1u} valence state of $16.5-17.0a_0^2$.[32] The values of about $90a_0^2$ for the $2^1B_{1u}(\pi,3p_y)$ Rydberg state and $11.7a_0^2$ for the ground-state calculated in this study indicate that the 1^1B_{1u} state of ethylene has a strong valence character and, thus, that Rydberg−valence mixing is limited.

Apart from the interaction between the (π,π^*) state and the $(\pi,3d_\pi)$ Rydberg state, other nonadiabatic coupling schemes have been suggested as well to explain the features and characteristics of the 6−8 eV absorption spectrum of ethylene. The absorption spectrum in this spectral range is traditionally attributed to vibronic transitions from the electronic ground state to the $1^1B_{1u}(\pi,\pi^*)$ valence state, with at the high-energy end superimposed sharp vibronic structure resulting from transitions to the $1^1B_{3u}(\pi,3s)$ Rydberg state.[9,20,33−40] A theoretical study of Siebrand et al.[13] suggested that the diffuse absorption bands of the $1^1B_{1u}(\pi,\pi^*) \leftarrow 1^1A_g$ spectrum in this region should be assigned to three kinds of ν_4 torsional progressions: (i) a "cold" 4_0^ν, (ii) a "hot" 4_1^ν, and (iii) a vibronically induced $i_0^1 4_0^\nu$ progression. A tentative proposal was made for the inducing mode of the latter progression as the nontotally symmetric ν_7 CH_2 wagging mode of b_{2g} symmetry.[41] This mode would allow coupling between the $1^1B_{1u}(\pi,\pi^*)$ valence state and the $1^1B_{3u}(\pi,3s)$ Rydberg state.

Petrongolo et al.[11,42] proposed that nonadiabatic coupling between the $1^1B_{1u}(\pi,\pi^*)$ valence and the $1^1B_{1g}(\pi,3p_y)$ Rydberg state is important to understand the spectroscopic properties of ethylene. Upon twisting of the CC double bond, both states will have the same symmetry and be mixed, ultimately leading to an avoided crossing. Ryu et al.[12] employed this coupling to explain the apparent inconsistency between the assignment of the electronic spectrum in the 5−8.5 eV energy region in terms of an $1^1B_{1u}(\pi,\pi^*)$ and $1^1B_{3u}(\pi,3s)$ excitation and the oscillator strengths calculated for these transitions. They come to the conclusion that the absorption spectrum in this energy region can be explained in terms of excitation of the coupled $1^1B_{1u}(\pi,\pi^*)$ and $1^1B_{1g}(\pi,3p_y)$ surfaces.

In the present work, we report the results of a two-photon excited-state photoelectron spectroscopic study of the $1^1B_{3u}(\pi,3s)$, $1^1B_{1g}(\pi,3p_y)$, $1^1B_{2g}(\pi,3p_z)$, and $2^1A_g(\pi,3p_x)$ Rydberg states within the 7−8.5 eV spectral range of both jet-cooled C_2H_4 and C_2D_4. The photoelectron spectra obtained here will be shown to confirm to a large extent previous assignments,[39,40] but with respect to the $(\pi,3p)$ Rydberg manifold, new assignments will be presented. Among else, it will be shown that the measured photoelectron spectra allow for the first time unambiguous assignments of the 0−0 two-photon transitions to all three $(\pi,3p)$ Rydberg states, providing a strikingly good agreement between the characteristics of the $(\pi,3p)$ Rydberg states as determined in the present study and in a previous ab initio study.[24] With regard to the $1^1B_{3u}(\pi,3s)$ Rydberg state, the photoelectron spectra enable us to conclude that a previous hypothesis that part of the two-photon $1^1B_{3u}(\pi,3s) \leftarrow 1^1A_g$ spectrum is vibronically induced via the $\nu_6(b_{1u})$ vibrational mode, coupling the $1^1B_{3u}(\pi,3s)$ Rydberg state and the Jahn−Teller distorted $1^1B_{2g}(\pi^*,3s)$ state,[40] is not correct. Instead, these photoelectron spectra demonstrate that the pertaining features can be readily associated with the $\nu_3(a_g)$ CH_2 scissors mode. Finally, the results will be considered in the light of Rydberg−valence and Rydberg−Rydberg coupling.

II. Experimental Details

The laser system and the magnetic bottle spectrometer used in the present study to perform the REMPI−PES experiments have been reported in detail elsewhere.[15,16] Briefly, excitation is done with a XeCl excimer laser (Lambda Physik EMG103MSC) working at a repetition rate of 30 Hz, which pumps a dye laser (Lumonics HyperDye-300) operating on RDC 360 Neu, PTP, DCM, Rhodamine B, or Rhodamine 6G. The output of this dye laser is frequency-doubled by an angle-tuned BBO or KDP crystal in an Inrad Autotracker II unit. The resulting excitation light has a spectral bandwidth of about 0.15 cm^{-1} and a pulse duration of about 15 ns. Typical maximum output after frequency-doubling is about 1−2 mJ per pulse. The excitation beam is steered into the magnetic bottle spectrometer and focused into the ionization region by a quartz lens with a focal length of 25 mm. The spectrometer consists of a "2π analyzer", based upon the original design by Kruit and Read,[43] which is equipped with a pulsed molecular beam. The laser pulse and molecular beam are synchronized by a home-built delay/pulse generator.

In the present experiments, the magnetic bottle spectrometer is employed exclusively in the electron detection mode. The 50% collection efficiency in this mode is achieved by a strongly diverging magnetic field in the ionization region that makes the trajectories of the produced photoelectrons parallel. The kinetic energies of these electrons are subsequently analyzed by means of a time-of-flight technique. After detection by a pair of microchannel plates, the signal is stored in a 500 MHz digital oscilloscope (Tektronix TDS540), which is read out by a computer. Typically, 90−150 time-of-flight spectra were averaged at each interval in an excitation and photoelectron scan.

The pulsed supersonic expansion is generated by a General Valve Iota One system. Expansion occurs into a chamber that is pumped by an Edwards Diffstak 2000 oil diffusion pump backed by an Edwards E2M40 rotary forepump. The expansion chamber is connected to the ionization chamber through a skimmer (Beam Dynamics) with a diameter of 0.5 mm. The orifice of the molecular beam can be variably set to a distance of 0−4.5 cm above the skimmer. In the present study, the expanded jet flow was collimated by the skimmer located typically 3.0 cm downstream of the valve orifice. The ionization region, located 20 cm below the skimmer, is evacuated by a Balzers TPH 170 turbomolecular pump backed by a Leybold Trivac D16B rotary forepump. The flight tube is pumped by a Leybold Turbovac 450 turbomolecular pump backed by a Leybold Trivac D25B rotary forepump.

Pulsed jet expansions have been created by expanding about 2 bar pure C_2H_4 (Hoek Loos, ethylene-h_4 3.0) and C_2D_4 (Aldrich, ethylene-d_4 99%) through a nozzle with a diameter of 500 μm into the expansion chamber. The pulse duration of typically 200 μs at a repetition rate of 30 Hz resulted in a pressure of about 1×10^{-4} mbar in the expansion chamber as measured with a Penning gauge (Edwards CP25-K). The pressure in the flight tube is not measurably dependent on the inlet of gas via the molecular beam system and is about 1×10^{-7} mbar as measured by a high vacuum ionization gauge (Leybold IE20).

III. Results and Discussion

Figure 1 shows the two-photon resonance enhanced excitation spectra of jet-cooled C_2H_4 and C_2D_4 recorded over the spectral

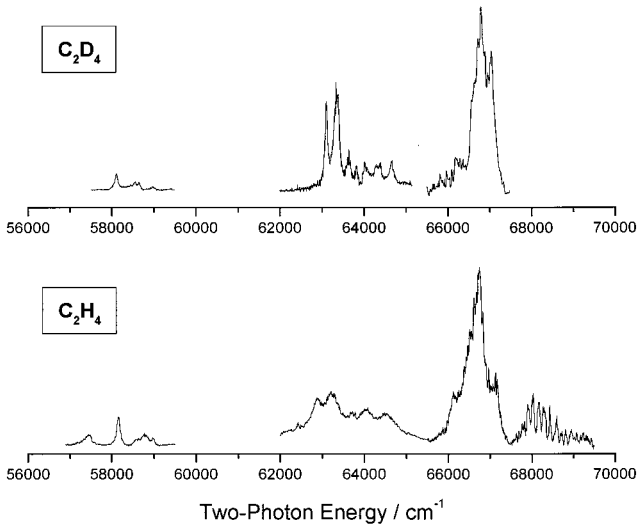

Figure 1. (2+1) REMPI excitation spectrum of jet-cooled C_2H_4 (bottom) and C_2D_4 (top) recorded over the two-photon energy range of 57 000−59 500 and 62 000−69 500 cm^{-1} showing resonances deriving from vibronic transitions to the $1^1B_{3u}(\pi,3s)$ state and the $(\pi,3p)$ Rydberg manifold, respectively.

ranges of 57 000−59 500 and 62 000−69 500 cm^{-1}. The electronically excited states investigated in this spectral region are the lowest excited Rydberg states, i.e., the $(\pi,3s)$ and $(\pi,3p)$ states. Because of the lack of enough laser power in the region between 59 500 and 62 000 cm^{-1}, this spectral region has been omitted in the present study. In comparison with the spectrum of jet-cooled C_2H_4 seeded in helium,[40] the present use of pure jet expansions does not seem to influence the line widths of the spectral features of C_2H_4. This is not the case for C_2D_4, where less well-resolved spectral features are obtained than for the helium-seeded expansions. As has been suggested previously,[40] this may be indicative of an enhanced predissociation in the excited states of C_2H_4 as compared to its deuterated isotopomer.

The nature of the features in Figure 1 has been investigated by recording photoelectron spectra at each of the resonances. These photoelectron spectra provide information on the internal energy of the radical cation formed in the resonant enhanced ionization process and, ultimately, about the (ro)vibronic nature of the excited-state level that is ionized. To be able to retrieve this information, it is essential to have detailed knowledge of the geometric and vibrational properties of the lowest ionic state. In the following, we will therefore first discuss the results of ab initio calculations that have been performed (section A), after which the results of these calculations will be used to assign the various resonances in the excitation spectra of C_2H_4 and C_2D_4 of the 3s Rydberg state (section B) and the 3p Rydberg states (section C). The results obtained from these analyzes will be discussed from the point of view of vibronic coupling in section D.

A. Ab Initio Calculations. Ab initio calculations have been performed at the (U)B3LYP/6-311G* level[44] employing the Gaussian suite of programs.[45] In ethylene, the ground state of the radical cation is associated with the removal of an electron from the highest occupied π orbital, leading to an ionic core with $^2B_{3u}$ symmetry in the D_{2h} point group. This symmetry notation assumes a planar geometry as is the case for ethylene in its electronic ground-state $S_0(1^1A_g)$,[10,46] but simulation of the vibrational features visible in the $D_0(1^2B_{3u}) \leftarrow S_0(1^1A_g)$ He(I) photoelectron spectra of C_2H_4 and C_2D_4 lead to the conclusion that the molecule adopts a partially twisted equilibrium geometry

TABLE 1: Geometrical Parameters (Angstroms and Degrees) of the Equilibrium Geometry for the $S_0(1^1A_g)$ Ground State of Neutral C_2H_4 and the $D_0(1^2B_{3u})$ Ground State of the Radical Cation Calculated at the (U)B3LYP/6-311G* Level[a]

	$S_0(1^1A_g)$		$D_0(1^2B_{3u})$	
parameter	experimental[b]	calculated	planar structure	twisted structure
r(C−C)	1.3391	1.3288	1.4184	1.3951
r(C−H)	1.0868	1.0859	1.0872	1.0903
∠(H−C−H)	117.44	116.32	118.29	117.52
∠(C═C−H)	121.28	121.84	120.85	121.24
τ(H−C═C−H)	0	0	0	26.74

[a] For D_0, both the planar structure of D_{2h} symmetry (1^2B_{3u}) as well as the twisted structure of D_2 symmetry (1^2B_3) has been optimized. [b] Experimental values from ref 46.

with a torsional angle of about 25° in the ground ionic state D_0.[47] This twisting around the CC bond has been explained by taking into account that the $D_0(1^2B_{3u})$ state is vibronically coupled to the first excited ionic state $D_1(2^2B_{3g})$ via the $\nu_4(a_u)$ vibrational mode. As a result, the potential energy surface of D_0 exhibits a pronounced anharmonicity with respect to this ν_4 mode. On the basis of poorly resolved He(I) photoelectron spectra, Köppel et al.[47] were proven right by subsequent well-resolved molecular beam He(I) photoelectron studies[48,49] on C_2H_4 and C_2D_4 in which a dihedral angle of 27° ± 2° was reported.

Our ab initio calculations of the geometry of the ground state of the radical cation under D_{2h} and D_2 constraints lead to the geometrical parameters reported in Table 1. The calculations reveal that the equilibrium structure of $C_2H_4^+$ has a dihedral angle of about 27°, which agrees very well with the previously reported experimental values.[47,48] It is also in good agreement with a CI calculation,[50] in which a dihedral angle of 25° was calculated. The calculated energy difference between the planar and twisted structure is about 235 cm^{-1}, once again in excellent agreement with previously obtained values of 270 ± 150 and 234 cm^{-1}.[48,47] This relatively low barrier for twisting around the CC bond implies that the *dynamic* symmetry of the molecule remains D_{2h}, although twisting lowers the *static* symmetry to D_2.

The harmonic force field calculated for the ground state of the radical cation at the twisted geometry gives rise to the vibrational frequencies reported in Table 2. To "calibrate" these calculations, we have also calculated the harmonic force field of the neutral ground state. The results of these calculations are given in Table 2 as well. It will turn out that the analysis of the 3s excitation region requires a good description of the ionic ν_2 and ν_3 coordinates. In the past there has been some discussion on a possible reversal of these coordinates upon ionization. This proposal was put forward on the basis of the observed line intensities in the He(I) photoelectron spectra of $C_2H_4^+$ and $C_2D_4^+$, and the notion that the Franck−Condon overlap for ν_2 should be significantly larger than for ν_3.[52] These assignments were supported in the assignments of highly resolved He(I) photoelectron spectra[48,49] of C_2H_4 and C_2D_4. McDiarmid[53] questioned these ν_2 and ν_3 assignments, because of the anomaly that would arise with the experimental evidence presented by the UV absorption spectrum of C_2H_4 and its deuterated analogues.[54] The issue was settled by SCF calculations on the geometry and harmonic force field of the ground state of the neutral and the radical cation in a planar equilibrium geometry.[51] Here it was argued that the original assignments for $C_2H_4^+$ were incorrect, and the observed difference in vibrational activity of

TABLE 2: Experimental and Calculated ((U)B3LYP/6-311G*) Vibrational Frequencies (cm^{-1}) of C_2H_4 (C_2D_4) in the $S_0(1^1A_g)$ Ground State of the Planar Neutral Molecule and the $D_0(1^1B_{3u})$ Ground State of the Twisted Radical Cation

			$S_0(1^1A_g)$		$D_0(1^2B_{3u})$	
$D_2h(D_2)$		assignment	expt[a]	calcd[b]	expt[c]	calcd[d]
$a_g(a)$	ν_1	CH str.	3026(2260)	3137(2323)		3016(2215)
	ν_2	CC str.	1630(1518)	1693(1572)	1494(1332)	1476(1318)
	ν_3	CH_2 scis.	1342(985)	1383(1006)	1264(961)	1239(952)
$a_u(a)$	ν_4	CH_2 twist	1023(726)	1059(749)	*e*	551(397)
$b_{1u}(b_1)$	ν_5	CH str.	3021(2200)	3122(2256)		3019(2194)
	ν_6	CH_2 scis.	1444(1078)	1481(1097)		1401(1044)
$b_2\ g(b_2)$	ν_7	CH_2 wag.	940(780)	962(796)		1045(864)
$b_{2u}(b_2)$	ν_8	CH str.	3105(2345)	3222(2398)		3130(2345)
	ν_9	CCH bend.	826(−)	841(604)		782(567)
$b_3\ g(b_3)$	ν_{10}	CH str.	3103(2310)	3193(2381)		3111(2338)
	ν_{11}	CCH bend.	1220(1011)	1248(1017)		1180(962)
$b_{3u}(b_3)$	ν_{12}	CH_2 wag.	949(720)	968(732)		876(666)

[a] Experimental frequencies obtained from ref 70. [b] Unscaled calculated values from the present study. [c] Experimental frequencies of $C_2H_4^+$ and $C_2D_4^+$ obtained from refs 48 and 49, respectively. [d] Calculated values have been scaled by 0.9715 (C_2H_4) and 0.9773 (C_2D_4). [e] Not reported because of strong anharmonicity (see text and Table 6.).

TABLE 3: Franck−Condon Factors and Duschinsky Matrix for the, in D_{2d}, Three Totally Symmetric Modes (a_g) and the Asymmetric ν_4 Torsional Mode (a_u) in C_2H_4 and C_2D_4 as Calculated from the Force Fields ((U)B3LYP/6-311G*) of the Ground State of the Neutral Planar Molecule and the Twisted Structure of the Lowest Radical Cation

		D_0 of C_2H_4						D_0 of C_2D_4			
		Duschinsky matrix						Duschinsky matrix			
S_0	int.[a]	$\nu_1(a_g)$	$\nu_2(a_g)$	$\nu_3(a_g)$	$\nu_4(a_g)$	S_0	int.[a]	$\nu_1(a_g)$	$\nu_2(a_g)$	$\nu_3(a_g)$	$\nu_4(a_g)$
$\nu_1(a_g)$	1.2	0.985	−0.056	0.045	0.156	$\nu_1(a_g)$	0.0	0.983	−0.018	0.139	−0.119
$\nu_2(a_g)$	53.1	0.025	**0.896**	**−0.354**	0.268	$\nu_2(a_g)$	130.1	0.109	**0.961**	**−0.089**	−0.237
$\nu_3(a_g)$	98.5	−0.015	**0.378**	**0.925**	−0.040	$\nu_3(a_g)$	18.1	−0.013	**0.080**	**0.995**	−0.054
$\nu_4(a_u)$		−0.169	−0.228	0.132	0.950	$\nu_4(a_u)$		0.148	0.224	0.036	0.963

[a] Intensities of the $(\nu_i)_0^1$ transitions are given relative to the intensity of the 0−0 transition, which is taken as 100.

ν_2 and ν_3 in the He(I) photoelectron spectrum of C_2H_4 and C_2D_4 was rationalized.

We have used the B3LYP/6-311G* force fields of the electronic ground state and the ground state of the radical cation of both C_2H_4 and its deuterated isotopomer to calculate the Duschinsky matrix and the Franck−Condon factors for absorption from S_0 to D_0. The results, summarized in Table 3 for the vibrational modes ν_1, ν_2, ν_3, and ν_4, which in D_2 symmetry are totally symmetric, show that for C_2H_4 significant mode scrambling between ν_2 and ν_3 occurs upon ionization. For C_2D_4, in contrast, these two modes are not mixed. The calculated Franck−Condon factors predict for C_2H_4 an intense 3_0^1 transition and a 2_0^1 transition with half the intensity of the 3_0^1 transition. For C_2D_4, this intensity ordering is reversed: an intense 2_0^1 transition is predicted and a small 3_0^1 transition. These predictions are in nearly quantitative agreement with the measured line intensities in the He(I) photoelectron spectra of C_2H_4 and C_2D_4.[48,49,52]

B. (π,3s) Rydberg State. Similar to the ground state of the radical cation and in agreement with theoretical studies,[18,22,24,50] ethylene has been shown to have a twisted geometry in the $1^1B_{3u}(3s)$ Rydberg state,[36,55] a dihedral angle of 25° and 37° has been reported,[36,55] and a low inversion barrier[36] of about 290 cm^{-1}. As a result of this low inversion barrier, tunneling occurs, and the effective symmetry of the molecule remains D_{2h}. The two-photon transition from the electronic ground state to the $1^1B_{3u}(3s)$ Rydberg state is therefore electronically forbidden but can be vibronically induced via the $\nu_4(a_u)$ torsional mode.[34,36,39,40,55] The twisting of the CC bond upon excitation to the $1^1B_{3u}(3s)$ Rydberg state is expected to lead to a dominant activity of ν_4 in the excitation spectrum of the 1^1B_{3u} state, as was indeed concluded in previous studies[36,39,40,55,56] and will be confirmed in the present study by excited-state photoelectron spectroscopy.

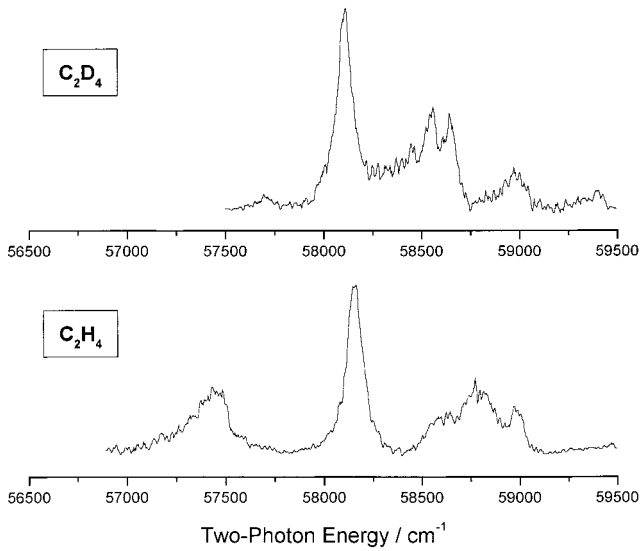

Figure 2. (2+1) REMPI excitation spectrum of jet-cooled C_2H_4 (bottom) and C_2D_4 (top) recorded over the two-photon energy range of 57 000−59 500 cm^{-1}, showing the resonances corresponding to the $1^1B_{3u}(\pi,3s) \leftarrow 1^1A_g$ transition.

The detailed (2+1) excitation spectrum of the $1^1B_{3u}(3s) \leftarrow 1^1A_g$ transition of C_2H_4 and C_2D_4 as measured in the present study with photoelectron detection is displayed in Figure 2. Assignments of the various resonances are given in Tables 4 and 5 for C_2H_4 and C_2D_4, respectively. The first observable resonances occur at 57 460 and 57 704 cm^{-1}, respectively, for the two molecules and have in the past been assigned as the 4_0^1 vibronically induced transition.[39,40] This assignment was based on selection rules (g ↔ u) and the energy spacing with respect to the 0−0 transition measured in one-photon absorption[36] and is confirmed by our photoelectron spectra obtained

TABLE 4: Assignments of Resonances in the Two-Photon Excitation Spectrum of the $1^1B_{3u}(\pi,3s)$ Rydberg State in C_2H_4

transition energy (cm^{-1})	relative energy (cm^{-1})		assignment		
		PES[b]	present study	Williams[c]	Gedanken[d]
57 338[a]	0		0_0^0	0_0^0	0_0^0
57 460	122	65	4_0^1	4_0^1	4_0^1
58 160	822	766	4_0^3	4_0^3	4_0^3
58 606	1268	1222	$3_0^1 4_0^1$	6_0^1	
58 796	1458	1545	4_0^5	$4_0^5 + 2_0^1 4_0^1$	$4_0^5 + 2_0^1 4_0^1$
58 985	1647	1574	$2_0^1 4_0^1$	$6_0^1 4_0^2$	

[a] Not observed in the present study. The transition energy of the 0−0 transition has been obtained from ref 36. [b] Kinetic energy of the photoelectrons corresponding to the dominant feature in the photoelectron spectrum (PES). [c] Assignment made by Williams and Cool.[40] [d] Assignment made by Gedanken et al.[39]

TABLE 5: Assignments of Resonances in the Two-Photon Excitation Spectrum of the $1^1B_{3u}(\pi,3s)$ Rydberg State in C_2D_4

transition energy (cm^{-1})	relative energy (cm^{-1})		assignment		
		PES[b]	present study	Williams[c]	Gedanken[d]
57 619[a]	0		0_0^0	0_0^0	0_0^0
57 704	85	*e*	4_0^1	4_0^1	4_0^1
58 108	489	500	4_0^3	4_0^3	4_0^3
58 450	831		?	6_0^1	
58 552	933	944	4_0^5	4_0^5	4_0^5
58 648	1029	1000	$3_0^1 4_0^1$	$6_0^1 4_0^2$	
58 980	1362		$2_0^1 4_0^1$	$2_0^1 4_0^1$	$2_0^1 4_0^1$

[a] Not observed in the present study. The transition energy of the 0−0 transition has been obtained from ref 36. [b] Kinetic energy of the photoelectrons corresponding to the dominant feature in the photoelectron spectrum (PES). [c] Assignment made by Williams and Cool.[40] [d] Assignment made by Gedanken et al.[39] [e] Not measurable because of spectral resolution.

at these excitation energies. We observe in the photoelectron spectrum taken at 57 460 cm^{-1} for C_2H_4 an intense peak shifted by about 8 meV, i.e., 65 cm^{-1}, from the energy expected for ionization to the vibrationless ground state of the radical cation. A similar shift is observed in photoelectron spectra taken at other resonances in the two-photon $1^1B_{3u} \leftarrow 1^1A_g$ excitation spectrum (vide infra). Although a frequency of 23 cm^{-1} was reported for the $\nu_4^+ = 1$ level of C_2D_4, it was not given for C_2H_4. A theoretical study predicted, however, a value of about

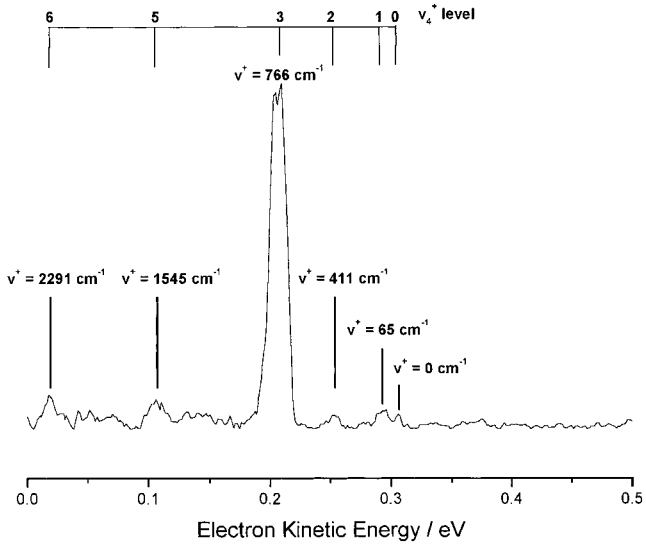

Figure 3. (2+1) REMPI photoelectron spectrum of C_2H_4 excited at 58 160 cm^{-1} showing predominant ionization to $v^+ = 766$ cm^{-1}, which corresponds to the $v_4^+ = 3$ level of D_0 of the radical cation. The photoelectron spectrum shows a distinct vibrational progression in ν_4, reflecting the strong anharmonicity of this vibrational mode in D_0.

100 cm^{-1}.[56] The experimentally observed spacing of about 65 cm^{-1} is in reasonable agreement with this value. For C_2D_4, the energy spacing of 23 cm^{-1} is below our experimental resolution, making it impossible to differentiate between ionization to the vibrationless level of the ion or to the $\nu_4^+ = 1$ level. Indeed, the photoelectron spectrum taken at 57 704 cm^{-1} is not at odds with the assignment of the resonance as 4_0^1.

Figure 3 shows a typical photoelectron spectrum of the $1^1B_{3u}(3s)$ state of C_2H_4, taken at 58 160 cm^{-1}. The strong feature in the spectrum corresponds to ionization to the $\nu_4^+ = 3$ level and confirms previous assignments[39,40] of the resonance as corresponding to the 4_0^3 transition. On either side of the dominant peak in the photoelectron spectrum, very weak sidebands can be observed that correspond to ionization to the $\nu_4^+ = 0$, 1, 2, 5, and 6 levels. Such weak sidebands involving $\Delta\mathbf{v} \neq 0$ ionization from the $1^1B_{3u}(3s)$ state to anharmonic levels of ν_4 in the ionic ground state are present in all photoelectron spectra taken at resonances in the two-photon $1^1B_{3u}(3s) \leftarrow 1^1A_g$ excitation spectra of C_2H_4 and C_2D_4, allowing us to determine and extend the frequencies of these levels up to $\nu_4^+ = 6$. These frequencies as well and those of the $1^1B_{3u}(3s)$ state are given in Table 6. Excellent agreement is observed between the present values and values reported in previous studies.[36,39,48,49,56]

TABLE 6: Observed and Calculated Anharmonic Torsional Energy Levels (cm^{-1}) of the ν_4 Vibrational Mode in the $1^1B_{3u}(\pi,3s)$ Rydberg State and the 1^2B_{3u} Ground State of the Radical Cation of C_2H_4 (C_2D_4)

	$1^1B_{3u}(\pi,3s)$ Rydberg state			1^2B_{3u} ground-state radical cation		
	experimental		calculated	experimental		calculated
ν_4 level	this study	previous studies	Chau[a]	this study	previous studies[b]	Chau[a]
0	*c*	0 (0)[d,e]	0 (0)	0 (0)	0 (0)	0 (0)
1	122 (85)	96 (41)[d]	113 (42)	65[f]	(23)	101 (35)
2		468 (286)[d]	464 (286)	411 (272)	438 (269)	438 (267)
3	822 (489)	820 (455)[e]	788 (474)	766 (500)	766 (503)	769 (451)
4		1084 (715)[d]	1162 (715)	(708)	1158 (715)	1158 (691)
5	1458 (933)	1500 (915)[e]	1550	1545 (944)		
6				2291		

[a] Calculated values have been obtained from ref 56. [b] Experimental values for $C_2H_4^+$ and $C_2D_4^+$ obtained from refs 48 and 49, respectively. [c] Not observed in the present (2+1) REMPI−PES study. [d] Experimental value obtained ref 36. [e] Experimental value obtained from ref 39. [f] $v_4^+ = 1$ level for C_2D_4 cannot be unambiguously determined from photoelectron spectrum because of spectral resolution.

Although these and other photoelectron spectra indicate that ionization from the $1^1B_{3u}(3s)$ state occurs for ν_4 with a predominant $\Delta\mathbf{v} = \mathbf{v}^+ - \mathbf{v}' = 0$ propensity, the presence of the sidebands indicates small changes in the CC twisting angle upon ionization. Taking this angle in the ground state of the radical cation around 25°−27°[47−50,56] suggests that the dihedral angle for the 1^1B_{3u} Rydberg state might be even larger. This would be in agreement with most experimental[36] and theoretical studies[18,22,24,50,56] that predict a torsional angle of about 25°−30° for the $1^1B_{3u}(3s)$ state. The significant higher value of about 37° predicted by Foo and Innes[55] seems, on the other hand, at odds with the present observations.

In the previous two-photon excitation studies,[39,40] the vibronic features in the two-photon excitation spectrum of the $1^1B_{3u}(3s)$ state were assigned in terms of vibronic transitions involving an odd number of quanta in ν_4 $\{4_0^1 - 4_0^3 - 4_0^5)$ in combination with progressions in the ν_2 CC stretching mode. Our excited-state photoelectron spectroscopy study confirms this Franck−Condon activity of the ν_4 torsional mode and of the ν_2 CC stretching mode. However, it shows at the same time that other resonances need to be reassigned. These concern in particular the resonances assigned to a new vibronic progression built upon the vibronically induced 6_0^1 transition.[40] This $\nu_6(b_{1u})$ CH_2 antisymmetric scissors mode was tentatively put forward to couple the $1^1B_{3u}(\pi,3s)$ Rydberg state with a state of B_{2g} symmetry for which several possibilities were proposed. Because in the present study we do not have as high laser powers available as in the study of Williams and Cool, we are only able to observe the resonances reported as 6_0^1 and $6_0^1 4_0^2$ at 58 606 (58 450) cm^{-1} in C_2H_4 (C_2D_4) and 58 985 (58 648) cm^{-1}, respectively. The shift in excitation energy of the 6_0^1 transition in C_2H_4 with respect to the previously reported number of 58 544 cm^{-1} can be attributed to the width of the resonances in the two-photon excitation spectrum of C_2H_4.

Focusing in first instance on the resonances in C_2H_4, the photoelectron spectrum taken at 58 606 cm^{-1} shows mainly ionization to an ionic level at 1222 cm^{-1}. Taking into account that our ab initio calculations predict a frequency of 1239 and 1401 cm^{-1} for $\nu_3(a_g)$ and $\nu_6(b_{1u})$, respectively, we can readily conclude that the transition at 58 606 cm^{-1} cannot be the 6_0^1 transition but must involve the ν_3 mode. Because this latter mode is totally symmetric and selection rules dictate that the parity of the vibrational state accessed from the totally symmetric ground state to the $1^1B_{3u}(3s)$ state should be odd, we assign the feature at 58 606 cm^{-1} to the $3_0^1 4_0^1$ transition. This would imply a frequency of 1146 and 1157 cm^{-1} for ν_3 in the $1^1B_{3u}(3s)$ Rydberg state and the ground state of the radical cation, respectively. Given the resolution in our photoelectron spectra, this is in good agreement with values reported in previous He(I) photoelectron studies[48] and the values calculated by us for the radical cation and by Mebel et al.[24] for the $1^1B_{3u}(3s)$ state. The photoelectron spectrum taken at the feature located at 58 985 cm^{-1}, previously assigned as the $6_0^1 4_0^2$ transition, shows mainly ionization to an ionic level at 1574 cm^{-1}. Using the same line of reasoning as before, we come to the conclusion that this transition should be assigned as the $2_0^1 4_0^1$ transition and that the frequency of ν_2 in the $1^1B_{3u}(3s)$ state and the ground state of the radical cation is 1525 and 1509 cm^{-1}, respectively. Within the experimental error, these values are in good agreement with the calculated and experimentally observed value for the radical cation[48] and the calculated value for the $1^1B_{3u}(3s)$ state.[24]

Assuming that the force fields and equilibrium geometries of the Rydberg states are to a large extent similar to those of the ground state of the radical cation, the Franck−Condon factors calculated for the $D_0 \leftarrow S_0$ transition (Table 3) predict that in the excitation spectrum of the $1^1B_{3u}(3s)$ state of C_2D_4 we should be able to see a clear $2_0^1 4_0^1$ transition, whereas the $3_0^1 4_0^1$ transition should have a small intensity. The previous assignment of the $2_0^1 4_0^1$ transition is indeed confirmed in the present study, but additionally, we find at 58 648 cm^{-1} a resonance that was previously assigned to the $6_0^1 4_0^2$ transition. In the present study, this resonance is superimposed upon a broad feature and seems to have a somewhat larger intensity than expected, but it is located at approximately the excitation energy anticipated for the $3_0^1 4_0^1$ transition. The associated photoelectron spectrum shows dominant ionization to an ionic vibrational level at 1000 cm^{-1}, which is in perfect agreement with the ionic frequencies of ν_3 and ν_4. The assignment of the feature at 58 648 cm^{-1} as the $3_0^1 4_0^1$ transition leaves the barely resolved feature at 58 450 cm^{-1} unassigned. In our excitation spectrum, this feature has such a low intensity that no decent photoelectron spectra could be recorded. Williams and Cool observed a well-resolved resonance at this position that was assigned as the 6_0^1 transition,[40] but the implied frequency of 831 cm^{-1} for ν_6 is at odds with the scaled ab initio value of 1044 cm^{-1}. At this moment, it is not clear, however, how this resonance should be assigned.

C. (π,3p) Rydberg States. The (π,3p) Rydberg states are two-photon allowed and have been observed in previous REMPI experiments.[39,40] Similar to the (π,3s) Rydberg state, ab initio studies[24,50] indicate that the (π,3p) Rydberg states have an elongated CC bond and twisted geometries. The most recent ones predict for the $1^1B_{1g}(\pi,3p_y)$ and $1^1B_{2g}(\pi,3p_z)$ Rydberg states a similar dihedral angle in the range of 10°−20° but a significantly larger angle of 34°−39° for the $2^1A_g(\pi,3p_x)$ Rydberg state.[24] On the basis of these geometric parameters, one may expect a dominant vibrational activity in the ν_4 torsional mode accompanied by progressions in the totally symmetric ν_2 CC stretch and ν_3 CH_2 scissors modes.

In the REMPI experiments of Gedanken et al.[39] and Williams and Cool,[40] the features at 62 900 (63 113) and 66 760 (66 840) cm^{-1} have been assigned as the 0−0 transitions from the electronic ground state to the (π,3p$_y$) and (π,3p$_x$) Rydberg states of C_2H_4 (C_2D_4), respectively. Williams and Cool assign all features observable in the 62 000−70 000 cm^{-1} spectral range to transitions to the (π,3p) Rydberg manifold, whereas Gedanken et al. assign some of them to vibronically induced transitions to the (π,3s) Rydberg state. A weak feature at 63 680 (63 831) cm^{-1} for C_2H_4 (C_2D_4) has been tentatively assigned as the 0−0 band to the (π,3p$_z$) Rydberg state.[40] From the polarization dependence of the resonances, Williams and Cool[40] could conclude that the highest-energy 0−0 transition in the (π,3p) Rydberg manifold belongs to the (π,3p$_x$) Rydberg state. This conclusion was reproduced in a large number of ab initio studies.[10,11,21,22,24,42,57] Most of these theoretical studies predicted that the $1^1B_{1g}(\pi,3p_y)$ and $1^1B_{2g}(\pi,3p_z)$ Rydberg states have nearly the same excitation energy, with a slightly lower excitation energy for the $1^1B_{1g}(\pi,3p_y)$ Rydberg state. The question about the order of these two states has therefore always been resolved in a rather arbitrary way, assuming the lower state to be the $1^1B_{1g}(\pi,3p_y)$ Rydberg state and the upper state to be the $1^1B_{2g}(\pi,3p_z)$ Rydberg state.[9,58] Recent ab initio calculations[24] on the vibronic spectra of the $1^1B_{1g}(\pi,3p_y)$ and $1^1B_{2g}(\pi,3p_z)$ Rydberg states suggest an opposite ordering, however.

Figure 4 shows the (2+1) REMPI excitation spectrum of the (π,3p) Rydberg manifold of C_2H_4 and C_2D_4. The corresponding assignments are reported in Tables 7 and 8, respectively. The

TABLE 7: Assignments of Resonances in the Two-Photon Excitation Spectrum of the (π,3p) Rydberg Manifold in C_2H_4

transition energy (cm^{-1})	relative energy (cm^{-1})	relative energy (cm^{-1})	relative energy (cm^{-1})	PES[a]	assignment $1^1B_{1g}(\pi,3p_y)$	assignment $1^1B_{2g}(\pi,3p_z)$	assignment $2^1A_g(\pi,3p_x)$
62 880	0			0	$3p_y0_0^0$		
63 236	356	0		444; 0	$3p_y4_0^2$	$3p_z0_0^0$	
63 720	840	484		460		$3p_z4_0^2$	
64 040	1160	804		1250	$3p_y4_0^4$		
64 520	1640	1284		1678; 1242	$3p_y3_0^14_0^2$	$3p_z4_0^4$	
66 120			0	0			$3p_x0_0^0$
66 748			628	387			$3p_x4_0^2$
67 150			1030	1121			$3p_x4_0^4$
67 896			1776				?
68 024			1904	1653; 1194			$3p_x3_0^14_0^2$
68 176			2056				$3p_x2_0^14_0^2$
68 284			2164				?
68 428			2308				$3p_x3_0^14_0^4$
68 604			2484				$3p_x2_0^14_0^4$
68 708			2588				$3p_x3_0^2$
68 816			2696				$3p_x2_0^13_0^1$
68 960			2840				$3p_x2_0^2$

[a] Kinetic energy of the photoelectrons corresponding to the dominant features in the photoelectron spectrum (PES).

TABLE 8: Assignments of Resonances in the Two-Photon Excitation Spectrum of the (π,3p) Rydberg Manifold in C_2D_4

transition energy (cm^{-1})	relative energy (cm^{-1})	relative energy (cm^{-1})	relative energy (cm^{-1})	PES[a]	Assignment $1^1B_{1g}(\pi,3p_y)$	Assignment $1^1B_{2g}(\pi,3p_z)$	Assignment $2^1A_g(\pi,3p_x)$
63 116	0			0	$3p_y0_0^0$		
63 368	252	0		295; 0	$3p_y4_0^2$	$\mathbf{3}p_z0_2^0$	
63 644	528	276		358		$3p_z4_0^2$	
63 832	716	464		750	$3p_y4_0^4$		
64 290	1174	922			$3p_y3_0^14_0^2$	$\mathbf{3}p_z3_0^1$	
64 384	1268	1016			$\mathbf{3}p_y2_0^1$		
64 668	1552	1300		1690; 1355	$3p_y2_0^14_0^2$	$\mathbf{3}p_z2_0^1$	
66 400			0	0			$3p_x0_0^0$
66 800			628	282			$3p_x4_0^2$
67 040			1030	718			$3p_x4_0^4$

[a] Kinetic energy of the photoelectrons corresponding to the dominant features in the photoelectron spectrum (PES).

photoelectron spectra recorded in the present study allow us to conclude that a number of transitions should be reassigned with respect to previous assignments.[39,40] If we first focus on the red side of the (2+1) REMPI excitation spectrum in Figure 4, we see that the features at 62 880 and 63 236 cm^{-1} for C_2H_4 (63 116 and 63 368 cm^{-1} for C_2D_4) need to be assigned as two origin bands. Figure 5 shows the photoelectron spectra for C_2H_4 recorded at these two positions. At 62 880 cm^{-1} a photoelectron spectrum is obtained with just one single peak deriving from ionization to the vibrationless level of the ion, and this resonance can therefore safely be assigned as a 0−0 transition. The photoelectron spectrum recorded at 63 236 cm^{-1} shows, on the other hand, two peaks corresponding with ionization to the vibrationless level of the ion and with the formation of ions with 444 cm^{-1} vibrational energy, which corresponds to the energy of the $v_4^+ = 2$ level. We assign the latter peak as deriving from (2+1) ionization via the 4_0^2 vibronic transition to the above-identified Rydberg state with its 0−0 transition at 62 880 cm^{-1}, whereas the former peak is associated with ionization of another (vibrationless) Rydberg state. On the basis of these two photoelectron spectra, the two bands at 62 880 and at 63 236 cm^{-1} are assigned as the origin transitions to the (π,3p_y) and (π,3p_z) Rydberg states. Because these two states are predicted to have a very similar geometry and vertical excitation energy, it is, however, impossible to differentiate between them on the basis of the excitation and photoelectron

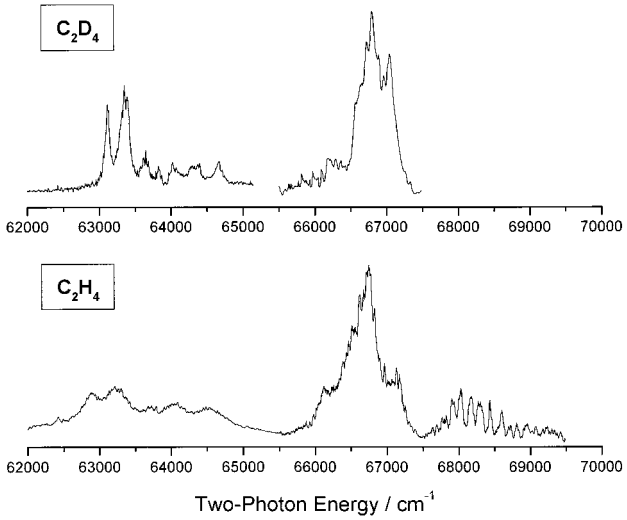

Figure 4. (2+1) REMPI excitation spectrum of jet-cooled C_2H_4 (bottom) and C_2D_4 (top) recorded over the two-photon energy range of 62 000−69 500 cm^{-1}, showing the vibronic transitions to the (π,3p) Rydberg manifold.

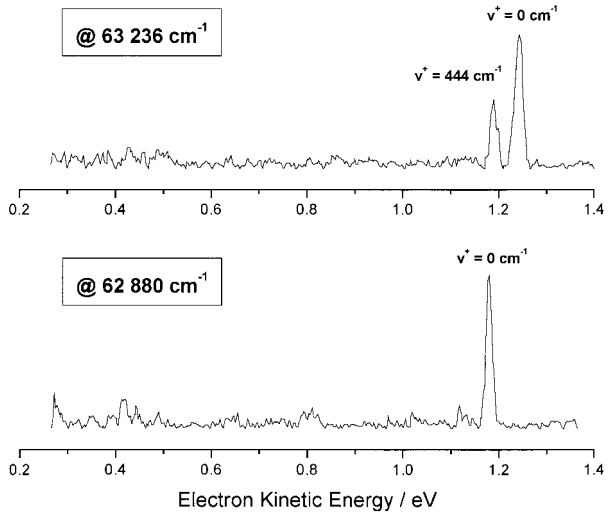

Figure 5. (2+1) REMPI photoelectron spectra of C_2H_4 excited at 62 880 (bottom) and 63 236 (top) cm^{-1}. The photoelectron spectrum taken at 62 880 cm^{-1} shows dominant ionization to $v^+ = 0$ cm^{-1} and is associated with ionization via the vibrationless level of either one of the quasidegenerate $1^1B_{1g}(\pi,3p_y)$ or $1^1B_{2g}(\pi,3p_z)$ Rydberg states. The photoelectron spectrum at 63 236 cm^{-1} shows ionization to $v^+ = 0$ and $v^+ = 444$ cm^{-1}, reflecting the electronic degeneracy of these two Rydberg states. These two ionization peaks correspond, respectively, to (i) ionization via the vibrationless levels of either one of these two $(\pi,3p)$ Rydberg states and (ii) ionization via the $\nu_4 = 2$ level in the $(\pi,3p)$ Rydberg state with its vibrationless level at 62 880 cm^{-1}.

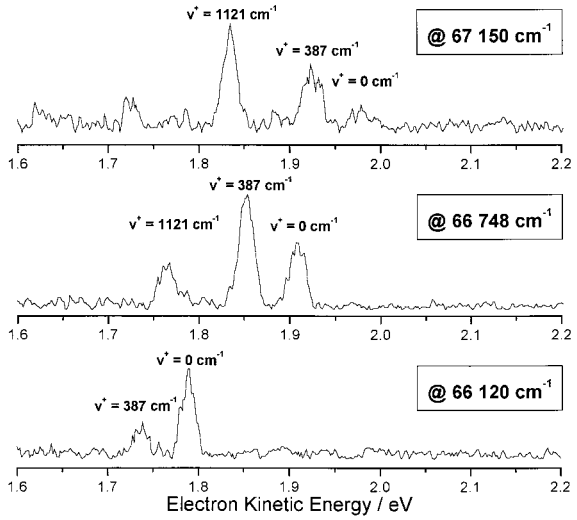

Figure 6. (2+1) REMPI photoelectron spectra of C_2H_4 excited at 66 120 (bottom), 66 748 (middle), and 67 150 (top) cm^{-1}. The bottom photoelectron spectrum shows predominant ionization to $v^+ = 0$ cm^{-1} and is associated with ionization via the vibrationless level of the $2^1A_g(\pi,3p_x)$ Rydberg state. The weaker signal at $v^+ = 387$ cm^{-1} is associated with ionization to the $v_4^+ = 2$ level in D_0 via the $\nu_4 = 2$ level of the $2^1A_g(\pi,3p_x)$ Rydberg state located at 66 748 cm^{-1} and is visible because of spectral overlap caused by lifetime broadening. For similar reasons, the photoelectron spectrum taken at 66 748 cm^{-1} shows, besides predominant ionization to $v^+ = 387$ cm^{-1}, also intense ionization to $v^+ = 0$ and 1121 cm^{-1}. The latter peak corresponds to ionization via the $\nu_4 = 4$ level of the $2^1A_g(\pi,3p_x)$ Rydberg state, a resonance that has its maximum at 67 150 cm^{-1}.

spectra. The calculations of Mebel et al. predict that the Franck−Condon factor for the 0−0 transition to the $(\pi,3p_y)$ state should be slightly larger than that of the 0−0 transition to the $(\pi,3p_z)$ state (0.5 vs. 0.4). This might argue for an assignment of the band at 62 880 cm^{-1} as the origin transition to the $(\pi,3p_y)$ state. The red side of the (2+1) REMPI excitation spectrum is composed of overlapping features belonging to vibronic transitions to the $(\pi,3p_y)$ and $(\pi,3p_z)$ Rydberg states. As Table 7 shows, these features can be readily (re)assigned by invoking the totally symmetric ν_2 and ν_3 modes as well as the asymmetric ν_4 torsional mode.

The second important reassignment emerging from the photoelectron spectra is that the strong feature at 66 748 cm^{-1} at the blue side of the excitation spectrum in Figure 4 does not correspond to the 0−0 transition to the $2^1A_g(\pi,3p_x)$ Rydberg state as was previously assumed.[39,40] Instead, it should be assigned as the 4_0^2 transition to this state. Figure 6 shows three photoelectron spectra recorded for C_2H_4 at 66120, 66748, and 67150 cm^{-1}. Going from the red to the blue side of the intense cluster of features between 66 000 and 67 500 cm^{-1}, we see that in each of the three photoelectron spectra an additional peak arises. The relatively weak feature at 66 120 cm^{-1} shows dominant ionization to the vibrationless level of the ion and is consequently assigned as an origin band, the 0−0 transition to the $2^1A_g(\pi,3p_x)$ Rydberg state. The photoelectron spectrum taken at 66 748 cm^{-1} shows dominant ionization to an ionic level at 387 cm^{-1}, assignable to the $\nu_4 = 2$ ionic level. This feature is therefore assigned as the 4_0^2 transition to the $2^1A_g(\pi,3p_x)$ Rydberg state. It might be argued that these two assignments imply that the $\nu_4 = 2$ level in the $2^1A_g(\pi,3p_x)$ Rydberg state has a frequency of about 628 cm^{-1}, which is significantly larger than that for the radical cation, but this difference is easily explained by taking into account the broadness of the line shapes of the resonance features in the (2+1) REMPI−PES excitation profile of C_2H_4, which is about 500 cm^{-1}. Finally, the feature at 67 150 cm^{-1}, 1030 cm^{-1} blue-shifted with respect to the 0−0 transition at 66 120 cm^{-1}, lead to dominant ionization to the $v_4^+ = 4$ level at 1121 cm^{-1} and is assigned as the 4_0^4 transition to the $2^1A_g(\pi,3p_x)$ Rydberg state.

Similar to the (2+1) REMPI excitation spectrum of the $1^1B_{3u}(\pi,3s)$ Rydberg state, the vibrational activity in the two-photon excitation spectrum of the $2^1A_g(\pi,3p_x)$ Rydberg state implies a rather large geometry change upon excitation from the electronic ground state because the 0−0 transition is much weaker than the 4_0^2 transition. Our revised assignments concurrently imply that for the other two $(\pi,3p)$ Rydberg states, where the 0−0 transition is dominant, the geometry changes are much less. This behavior of the ν_4 torsional mode suggests that the $2^1A_g(\pi,3p_x)$ Rydberg state is significantly more twisted around the CC bond than the $1^1B_{1g}(\pi,3p_y)$ and $1^1B_{2g}(\pi,3p_z)$ Rydberg states, which would be in agreement with previous ab initio calculations[24] that predict a significantly larger dihedral angle for the $(\pi,3p_x)$ than for the $(\pi,3p_y)$ and $(\pi,3p_z)$ Rydberg states. In these calculations, a Franck−Condon pattern is obtained for the $(\pi,3p_y)$ and $(\pi,3p_z)$ Rydberg states with the 0−0 transition as the strongest feature, whereas for the $(\pi,3p_x)$ Rydberg state, the 4_0^2 transition has the most intensity with the 0−0 transition roughly 10 times weaker. All of these predictions are in perfect agreement with the present experimental observations.

In our study employing pure jet expansions of C_2H_4, we obtain in the 67 800−69 000 cm^{-1} region an excitation spectrum with reasonably well-resolved features. An interesting observation, for which we do not have an explanation at the moment, is that in the previous study using helium-seeded C_2H_4 jet expansions considerably less well-resolved spectra were obtained in this energy region.[40] Most of the resonant features in the 67 800−69 000 cm^{-1} region of C_2H_4 can be readily assigned on the basis of their energy relative to the origin transition to the $2^1A_g(\pi,3p_x)$ Rydberg state at 66 120 cm^{-1}. These assign-

ments are listed in Table 7 and can be associated with vibronic transitions to the $2^1A_g(\pi,3p_x)$ Rydberg state involving the totally symmetric ν_2 and ν_3 modes, whether in combination with even quanta in the ν_4 torsional mode. Confirmation of the proposed assignments by photoelectron spectral analysis was not possible because the ionization signals giving rise to the excitation profile of C_2H_4 in the 67 800−69 000 cm^{-1} region are too weak to allow dispersion of the photoelectrons according to their kinetic energy. This signal-to-noise ratio was even worse for C_2D_4 for which we were even unable to record any excitation profile in this region at all.

D. Rydberg−Valence and Rydberg−Rydberg Coupling. Traditionally, the one-photon absorption spectrum of C_2H_4 in the 6−8 eV region is attributed to the excitation of the $1^1B_{1u}(\pi,\pi^*)$ valence state with, starting from 57 338 cm^{-1} (about 7.1 eV), superimposed excitation of the $1^1B_{3u}(\pi,3s)$ Rydberg state.[9,20,33−37] Several ab initio studies[11−13,18,42] investigating the characteristics of the long torsional progression of the ν_4 vibrational mode in the excitation spectrum of the $1^1B_{1u}(\pi,\pi^*)$ valence state[33,55,58−62] have stressed that nonadiabatic coupling effects between the valence state and the Rydberg manifold should be taken into account in order to explain the vibronic features observed in the 6−8 eV region of the absorption spectrum of ethylene.

Buenker and Peyerimhoff and others[11,12,18,42] have explained the observed spectral intensity distribution in the 6−8 eV region in terms of nonadiabatic coupling between the $1^1B_{1u}(\pi,\pi^*)$ valence state and the $1^1B_{1g}(\pi,3p_y)$ Rydberg state. These two excited singlet states are involved in configuration mixing upon a torsional movement around the CC bond, because for a twisted geometry of ethylene the symmetry of both states is lowered to $^1B_1$. As a consequence of this Rydberg−valence coupling effect, two excited singlet states are obtained. At the planar geometry, i.e., within the Franck−Condon region, the lower state, designated as the R/V state, has primarily Rydberg character and the upper state, designated as the V/R state, has dominant valence character. Twisting around the CC bond ultimately leads around the avoided crossing between the excited-state potentials of the two states to a switch of the electronic character: the (π,π^*) valence character of the upper (V/R) state is traded in for Rydberg character, and the lower (R/V) state loses its $(\pi,3p_y)$ Rydberg character and gains (π,π^*) valence character.

According to Ryu and Hudson,[12] the two-photon excitation spectrum of ethylene[39,40] can also be explained in this picture. This conclusion is not reflected in the present results. The photoelectron spectra in the 7−8.5 eV region show two important features concerning the electronic properties of the vibronically excited states responsible for the spectral features in this region. First, all of the photoelectron spectra indicate conservation of internal energy upon ionization of the intermediate vibronically excited states; that is, the dominant feature in the spectra corresponds to $\Delta\mathbf{v} = 0$. This ionization behavior is typical for "pure" Rydberg states. Second, the (2+1) photoelectron spectra present unambiguous evidence for three 0−0 transitions at 62 880, 63 236, and 66 120 cm^{-1} and one vibronically induced transition whose 0−0 transition is at 57 338 cm^{-1}.[36] On the basis of these experimental findings, one has to conclude that the vibronic features in the spectral range from 57 300 to 69 000 cm^{-1}, as studied by resonance enhanced multiphoton ionization, are associated with excitations from the electronic ground state to four separate excited singlet states that are predominantly of Rydberg character with quantum defects δ of about 1, 0.76, 0.74, and 0.58, i.e., the $1^1B_{3u}(\pi,3s)$, $1^1B_{1g}(p,3p_y)$, $1^1B_{2g}(\pi,3p_z)$, and $2^1A_g(\pi,3p_x)$ Rydberg states, respectively.

Some further consideration of these results is, however, necessary. In particular, a question to be answered is to what extent the photoelectron spectra obtained in the present study are able to provide a direct spectroscopic reflection of a possibly mixed character of the excited state caused by coupling between the Rydberg manifold and the (π,π^*) valence state. How effectively ionization from these states proceeds, depends on both the electronic transition moment from the excited state to the ionization continuum, the vibrational overlap between nuclear wave functions in the excited and ionic states, and the lifetime of the intermediate state. With respect to the electronic transition moment, the one-photon oscillator strength of a valence state is considerably larger than that of a Rydberg state. This dominance of the electronic transition moment may, however, be completely overshadowed by highly unfavorable Franck−Condon factors. This will especially be the case for valence states where significant molecular rearrangements or even molecular decomposition occurs. In contrast, the potential energy surface and equilibrium geometry of Rydberg states and that of their ionic core are in general very similar and will thus give rise to favorable Franck−Condon factors.

In the case of ethylene, it has been shown experimentally and theoretically that the relaxed equilibrium geometry of the $1^1B_{1u}(\pi,\pi^*)$ valence state of ethylene[10,11,21−24] is characterized by twisting one of the CH_2 groups by 90°, resulting in a large difference between the vertical and adiabatic excitation energies of this state: calculated values between 1.5 and 2.5 eV have been reported.[23,24] Highly unfavorable Franck−Condon factors for excitation to and ionization from this valence state can thus be anticipated. This has been illustrated in an ab initio study by Mebel et al.,[24] who concluded that the $1^1B_{1u}(\pi,\pi^*)$ valence state merely constitutes an underlying continuum of vibronic states with superimposed relatively strong Rydberg excitations. In an uncoupled picture, multiphoton ionization of the $1^1B_{1u}(\pi,\pi^*)$ valence state may therefore be expected to start to proceed efficiently if there is an excess energy available in the photoionization process of about 1.5−2.5 eV. For the currently employed one-color two-photon excitation scheme, this implies that ionization of $1^1B_{1u}(\pi,\pi^*)$ valence state character requires the absorption of an additional two photons; that is, (2+2) photoionization is necessary. Apart from the vibrational overlap argument, it is possible that experimental evidence of Rydberg−valence coupling is disguised by dynamic processes: femtosecond pump−probe studies on jet-cooled ethylene excited at 6 eV reveal a lifetime of about 20−30 fs.[64,65] Overall, we have to conclude therefore that, although excited-state photoelectron spectroscopy is in general a technique excellently suited for the disentanglement of coupled states, Rydberg−valence coupling may in the present case be hard to detect. One unambiguous signature would be (2+2) ionization. In similar studies on TME and BCH, such (2+2) "valence" signals have indeed been found,[4] but for ethylene, any ionization signal that can be attributed to the valence state has not been observed even at our highest laser powers.

The arguments given above for coupling of valence and Rydberg states lead one to expect that coupling *within* the Rydberg manifold, e.g., Rydberg−Rydberg coupling between the $(\pi,3s)$ and $(\pi,3p)$ Rydberg states, should be immediately apparent from the present photoelectron spectra. As an example, we will focus on the 0−0 transitions to the three $(\pi,3p)$ Rydberg states at 62 880, 63 236, and 66 120 cm^{-1} (63 116, 63 368, and 66 400 cm^{-1}) for C_2H_4 (C_2D_4). If any of the three $(\pi,3p)$

Rydberg states would be vibronically coupled to the (π,3s) Rydberg state at 57 338 (57 619) cm^{-1} for C_2H_4 (C_2D_4), then the photoelectron spectra taken at the 0−0 transitions of the (π,3p) states should show an ionization signal from highly vibrationally excited levels of the (π,3s) state corresponding to ions with an internal vibrational energy of 0.716, 0.731, and 1.089 eV, respectively (0.682, 0.713, 1.089 eV for C_2D_4). This is not the case as becomes clear, for example, from the spectra in Figure 5 where the photoelectron spectra recorded at the 0−0 transitions to the $1^1B_{1g}(\pi,3p_y)$ and $1^1B_{2g}(\pi,3p_z)$ Rydberg states are shown. No photoelectrons associated with kinetic energies of 0.493 and 0.515 eV, respectively, are observed. Similar arguments demonstrate that vibronic coupling between the three (π,3p) Rydberg states is also absent or, at least, not visible in the present experiments.

The present observation that the lower Rydberg states in ethylene are not directly or even indirectly, via the vibronic valence continuum underlying these Rydberg states, vibronically coupled to each other may seem insignificant. However, it will prove to be important when the photophysics of ethylene are compared with those of its methyl-substituted derivatives such as tetramethylethylene[4,66,67] and larger monoolefinic compounds, such as 1,1′-bicyclohexylidene,[4−6] and mono-olefinic steroids[68] with a single isolated CC double bond. A recent excited-state photoelectron spectroscopy study on jet-cooled tetramethylethylene and as 1,1′-bicyclohexylidene[4] has shown that substitution of the four protons in ethylene has a dramatic effect on the spectroscopy and dynamics as reflected in the photoelectron spectra: the photophysics of these highly substituted ethylene derivatives are completely dominated by Rydberg−Rydberg and/or Rydberg−valence coupling. Both experimental[4] and theoretical evidence[69] for the rather different nature of the spectroscopy and dynamics of these larger monoolefinic molecules, as compared to their chromophore ethylene, will shortly be reported.

IV. Conclusions

Excited-state photoelectron spectroscopy, allowing for the dispersion of the kinetic energies of the photoelectrons produced in a REMPI excitation scheme, is an invaluable tool to elucidate the nature of vibronic transitions. In the present study on jet-cooled ethylene, this spectroscopic technique has proven to be very adequate: for the first time, the 0−0 transitions to all three (π,3p) Rydberg states in both C_2H_4 and its deuterated isotopomer could be assigned unambiguously on the basis of the recorded photoelectron spectra. The overlapping vibronic structure in the "high-resolution" (2+1) REMPI excitation spectrum of jet-cooled C_2H_4 and C_2D_4 of the quasidegenerate $1^1B_{1g}(\pi,3p_y)$ and $1^1B_{2g}(\pi,3p_z)$ Rydberg states has been disentangled and assigned. Although our studies do not allow the order of the two states to be established, they do show that the (π,3p$_y$) and (π,3p$_z$) states have similar vibronic spectra. In contrast to previous multiphoton studies on ethylene,[39,40] the present excited-state photoelectron spectroscopy study shows that the 0−0 transition to the $2^1A_g(\pi,3p_x)$ Rydberg state is not associated with the most intense feature in the (2+1) REMPI excitation spectrum but corresponds to a much weaker feature. The origin transition as assigned before has been identified as the first member of a progression in the ν_4 torsional mode. The consequence of the present assignments is that one has to conclude that the equilibrium geometry of the $2^1A_g(\pi,3p_x)$ state is changed more upon excitation from the electronic ground state than the other two (π,3p) states.

Most of the previous assignments of the vibronic features in the (2+1) REMPI excitation spectrum of the $1^1B_{3u}(\pi,3s)$ Rydberg state have been confirmed. However, a rather tentative proposal[40] to assign part of this spectrum as vibrationally induced by coupling of the $1^1B_{3u}(\pi,3s)$ Rydberg state to the Jahn−Teller distorted $1^1B_{2g}(\pi^*,3s)$ state[36] via the ν_6 CH_2 antisymmetric scissors mode of b_{1u} symmetry is rejected. Instead, the present photoelectron spectra show that these features are associated with the totally symmetric ν_3 CH_2 scissors mode. The vibrational activity of the ν_3 mode is indeed to be expected from previous[51] and present ab initio calculations that indicate significant mode scrambling of the totally symmetric ν_2 C═C stretching and the ν_3 CH_2 scissors mode upon excitation from the ground state to the Rydberg manifold.

Excited-state photoelectron spectroscopy is generally an excellent means to unravel the nature of an electronically excited state, e.g., Rydberg versus valence character. For ethylene, it has been argued that very unfavorable Franck−Condon factors[23,24] and highly efficient relaxation processes associated with the specific $1^1B_{1u}(\pi,\pi^*)$ valence state[64,65] may heavily impede ionization from this valence shell configuration. Although a possible signature for this ionization has been suggested and was indeed observed in studies on substituted ethylenes, the bare molecule still seems to resist detailed studies of ideas put forward in the literature on coupling between the $1^1B_{1u}(\pi,\pi^*)$ valence state and the $1^1B_{3u}(\pi,3s)$[13] or the $1^1B_{1g}(\pi,3p_y)$ Rydberg state[11,12,18,42] by these means. However, the present study reveals without doubt that there is no significant Rydberg−Rydberg vibronic coupling within the lower Rydberg manifold of ethylene.

Acknowledgment. We gratefully acknowledge Ing. D. Bebelaar for valuable technical assistance and Prof. Dr. C. A. de Lange and Prof. Dr. M. Glasbeek for the use of equipment.

References and Notes

(1) Oosterbaan, W. D.; Havenith, R. W. A.; van Walree, C. A.; Jenneskens, L. W.; Gleiter, R.; Kooijman, H.; Spek, A. L. *J. Chem. Soc., Perkin Trans. 2* **2001**, 1066.

(2) Hoogesteeger, F. J.; Havenith, R. W. A.; Zwikker, J. W.; Jenneskens, L. W.; Kooijman, H.; Veldman, N.; Spek, A. L. *J. Org. Chem.* **1995**, *60*, 4375.

(3) Hoogesteeger, F. J.; van Walree, C. A.; Jenneskens, L. W.; Roest, M. R.; Verhoeven, J. W.; Schuddeboom, W.; Piet, J. J.; Warman, J. M. *Chem. Eur. J.* **2000**, *6*, 2948.

(4) Rijkenberg, R. A.; Buma, W. J.; van Walree, C. A.; Jenneskens, L. W. To be published.

(5) Snyder, P. A.; Clark, L. B. *J. Chem. Phys.* **1970**, *52*, 998.

(6) Allan, M.; Snyder, P. A.; Robin, M. B. *J. Phys. Chem.* **1985**, *89*, 4900.

(7) Mulliken, R. S. *Chem. Phys. Lett.* **1977**, *46*, 197.

(8) Buenker, R. J.; Peyerimhoff, S. D. *Chem. Phys. Lett.* **1975**, *36*, 415.

(9) Robin, M. *Higher Excited States of Polyatomic Molecules*; Academic Press: New York, 1985; Vol III.

(10) Wiberg, K. B.; Hadad, C. M.; Foresman, J. B.; Chupka, W. A. *J. Phys. Chem.* **1992**, *96*, 10756.

(11) Petrongolo, C.; Buenker, R. J.; Peyerimhoff, S. D. *J. Chem. Phys.* **1982**, *76*, 3655.

(12) Ryu, J.; Hudson, B. S. *Chem. Phys. Lett.* **1995**, *245*, 448.

(13) Siebrand, W.; Zerbetto, F.; Zgierski, M. Z. *Chem. Phys. Lett.* **1990**, *174*, 119.

(14) Langford, S. R.; Orr-Ewing, A. J.; Morgan, R. A.; Western, C. M.; Ashfold, M. N. R.; Rijkenberg, R. A.; Scheper, C. R.; Buma, W. J.; de Lange, C. A. *J. Chem. Phys.* **1998**, *108*, 6667.

(15) Rijs, A. M.; Backus, E. H. G.; de Lange, C. A.; Westwood, N. P. C.; Janssen, M. H. M. *J. Electron Spectrosc. Relat. Phenom.* **2000**, *112*, 151.

(16) Scheper, C. R.; Buma, W. J.; de Lange, C. A. *J. Electron Spectrosc. Relat. Phenom.* **1998**, *97*, 147.

(17) Johnson, P. M. *Acc. Chem. Res.* **1980**, *13*, 20.

(18) Peyerimhoff, S. D.; Buenker, R. J. *Theor. Chim. Acta* **1972**, *27*, 243.

(19) Buenker, R. J.; Peyerimhoff, S. D. *Chem. Phys. Lett.* **1971**, *11*, 65.

(20) Mulliken, R. S. *J. Chem. Phys.* **1977**, *66*, 2448.

(21) McMurchie, L. E.; Davidson, E. R. *J. Chem. Phys.* **1977**, *67*, 5613.
(22) Foresman, J. B.; Head-Gordon, M.; Pople, J. A.; Frisch, M. J. *J. Phys. Chem.* **1992**, *96*, 135.
(23) Mebel, A. M.; Chen, Y.-T.; Lin, S. H. *Chem. Phys. Lett.* **1996**, *258*, 53.
(24) Mebel, A. M.; Chen, Y.-T.; Lin, S. H. *J. Chem. Phys.* **1996**, *105*, 9007.
(25) Bender, C. F.; Dunning, T. H., Jr.; Schaefer, H. F., III.; Goddard, W. A., III.; Hunt, W. J. *Chem. Phys. Lett.* **1972**, *15*, 171.
(26) McMurchie, L. E.; Davidson, E. R. *J. Chem. Phys.* **1977**, *66*, 2959.
(27) Brooks, B. R.; Schaefer, H. F., III. *J. Chem. Phys.* **1978**, *68*, 4839.
(28) Davidson, E. R. *J. Phys. Chem.* **1996**, *100*, 6161.
(29) Lindh, R.; Roos, B. O. *Int. Quantum Chem.* **1989**, *35*, 813.
(30) Krebs, S.; Buenker, R. J. *J. Chem. Phys.* **1997**, *106*, 7208.
(31) Buenker, R. J.; Shih, S.-K.; Peyerimhoff, S. D. *Chem. Phys.* **1979**, *36*, 97.
(32) Müller, T.; Dallos, M.; Lischka, H. *J. Chem. Phys.* **1999**, *110*, 7176.
(33) Wilkinson, P. G.; Mulliken, R. S. *J. Chem. Phys.* **1955**, *23*, 1895.
(34) Merer, A. J.; Mulliken, R. S. *Chem. Rev.* **1969**, *69*, 639.
(35) Merer, A. J.; Mulliken, R. S. *J. Chem. Phys.* **1969**, *50*, 1026.
(36) Merer, A. J.; Schoonveld, L. *Can. J. Phys.* **1969**, *47*, 1731.
(37) Merer, A. J.; Schoonveld, L. *J. Chem. Phys.* **1968**, *48*, 533.
(38) Mulliken, R. S. *J. Chem. Phys.* **1979**, *71*, 556.
(39) Gedanken, A.; Kuebler, N. A.; Robin, M. B. *J. Chem. Phys.* **1982**, *76*, 46.
(40) Williams, B. A.; Cool, T. A. *J. Chem. Phys.* **1991**, *94*, 6358.
(41) In the study of Siebrand et al.,[13] a different vibrational numbering was employed based upon D_2 symmetry. In this point group, the CH_2 wagging mode becomes ν_8.
(42) Petrongolo, C.; Buenker, R. J.; Peyerimhoff, S. D. *J. Chem. Phys.* **1983**, *78*, 7284.
(43) Kruit, P.; Read, F. H. *J. Phys. E* **1983**, *16*, 313.
(44) Becke, A. D. *J. Chem. Phys.* **1993**, *98*, 5648.
(45) Frisch, M. J.; Trucks, G. W.; Schlegel, H. B.; Scuseria, G. E.; Robb, M. A.; Cheeseman, J. R.; Zakrzewski, V. G.; Montgomery, J. A.; Stratmann, R. E.; Burant, J. C.; Dapprich, S.; Millam, J. M.; Daniels, A. D.; Kudin, K. N.; Strain, M. C.; Farkas, O.; Tomasi, J.; Barone, V.; Cossi, M.; Cammi, R.; Mennuci, B.; Pomelli, C.; Adamo, C.; Clifford, S.; Ochterski, J.; Petersson, G. A.; Ayala, P. Y.; Cui, Q.; Morokuma, K.; Malick, D. K.; Rabuck, A. D.; Raghavachari, K.; Foresman, J. B.; Cioslowski, J.; Ortiz, J. V.; Baboul, A. G.; Stefanov, B. B.; Liu, G.; Liashenko, A.; Piskorz, P.; Komaromi, I.; Gomperts, R.; Martin, R. L.; Fox, D. J.; Keith, T.; Al-Laham, M. A.; Peng, C. Y.; Nanayakkara, A.; Gonzalez, C.; Challacombe, M.; Gill, P. M. W.; Johnson, B.; Chen, W.; Wong, M. W.; Andres, J. L.; Gonzalez, C.; Head-Gordon, M.; Repogle, E. S.; Pople J. A., *Gaussian 98*, revision A.7; Gaussian, Inc.: Pittsburgh, PA, 1998.
(46) Callomon, J. H.; Horota, E.; Iijima, T.; Kuchitsu, K.; Lafferty, J. W. *New Series, Group II(15)*; Springer-Verlag: Berlin, 1987.
(47) Köppel, H.; Domcke, W.; Cederbaum, L. S.; von Niessen, W. *J. Chem. Phys.* **1978**, *69*, 4252.
(48) Pollard, J. E.; Trevor, D. J.; Reutt, J. E.; Lee, Y. T.; Shirley, D. A. *J. Chem. Phys.* **1984**, *81*, 5302.
(49) Wang, L.; Pollard, J. E.; Lee, Y. T.; Shirley, D. A. *J. Chem. Phys.* **1987**, *86*, 3216.
(50) Buenker, R. J.; Peyerimhoff, S. D.; Hsu, H. L. *Chem. Phys. Lett.* **1971**, *11*, 65.
(51) Somasundram, K.; Handy, N. C. *J. Chem. Phys.* **1986**, *84*, 2899.
(52) Cvitaš, T.; Güsten, H.; Klasinc, L. *J. Chem. Phys.* **1979**, *70*, 57.
(53) McDiarmid, R. *J. Chem. Phys.* **1985**, *83*, 3174.
(54) McDiarmid, R. *J. Phys. Chem.* **1980**, *84*, 64.
(55) Foo, P. D.; Innes, K. K. *J. Chem. Phys*. **1974**, *60*, 4582.
(56) Chau, F. T. *J. Mol. Struct.* **1985**, *131*. 383.
(57) Nakatsuji, H. *J. Chem. Phys.* **1984**, *80*, 3703.
(58) McDiarmid, R. *Advances in Chemical Physics*; John Wiley & Sons: New York, 1999; Vol. 110.
(59) McDiarmid, R. *J. Chem. Phys.* **1969**, *50*, 1794.
(60) Warshel, A.; Karplus, M. *Chem. Phys. Lett.* **1972**, *17*, 7.
(61) Wilkinson, P. G. *J. Mol. Spectrosc.* **1961**, *6*, 1.
(62) McDiarmid, R.; Charney, E. *J. Chem. Phys.* **1967**, *47*, 1517.
(63) McDiarmid, R. *J. Chem. Phys.* **1971**, *55*, 4669.
(64) Farmanara, P.; Stert, V.; Radloff, W. *Chem. Phys. Lett.* **1998**, *298*, 57.
(65) Mestdagh, J. M.; Visticot, J. P.; Elhanine, M.; Soep, B. *J. Chem. Phys.* **2000**, *113*, 237.
(66) Snyder, P. A.; Hansen, R. W. C. Rowe, E. M. *J. Phys. Chem.* **1996**, *100*, 17756.
(67) Robin, M. B.; Hart, R. R. Kuebler, N. A. *J. Chem. Phys.* **1966**, *44*, 1803.
(68) Yogev, A.; Sagiv, J.; Mazur, Y. *J. Am. Chem. Soc.* **1972**, *94*, 5122.
(69) Rijkenberg, R. A.; Buma, W. J.; van Walree, C. A.; Jenneskens, L. W.; Schmal, L. P.; van Lenthe, J. H. To be published.
(70) Duncan, J. L.; McKean, D. C.; Mallinson, P. D. *J. Mol. Spectrosc.* **1973**, *45*, 221.